**EARTH'S CRYOSPHERE**
SCIENTIFIC JOURNAL

*Earth's Cryosphere*, 2024, vol. XXVIII, No. 5, pp. 3–11

*REGIONAL AND HISTORICAL GEOCRYOLOGY*

# NEW DATA ON THE GEOCHRONOLOGY OF QUATERNARY SEDIMENTS AND STABLE OXYGEN AND HYDROGEN ISOTOPES IN GROUND ICE OF THE MAMONTOVA GORA

**N.V. Torgovkin[1, *], D.E. Sivtsev[1,2], A.A. Gavrilova[3], I.A. Platonov[2], A.I. Kizyakov[2], L. Schirrmeister[4], T. Opel[4], S. Wetterich[5], S.F.M. Breitenbach[6], H. Meyer[4]**

[1] *Melnikov Permafrost Institute, Siberian Branch of the Russian Academy of Sciences, Merzlotnaya St. 36, Yakutsk, 677010 Russia*
[2] *Lomonosov Moscow State University, Faculty of Geography, Leninskie Gory 1, Moscow, 119991 Russia*
[3] *Institute of Precambrian Geology and Geochronology, Russian Academy of Sciences, Makarova St. 2, St. Petersburg, 199034 Russia*
[4] *Alfred Wegener Institute, Helmholtz Center for Polar and Marine Research, 14473 Potsdam, Germany*
[5] *Institute of Geography, Dresden University of Technology, 01069 Dresden, Germany*
[6] *Department of Earth and Environmental Sciences, Northumbria University, Newcastle-Upon-Tyne, NE1 8ST, United Kingdom*

**Corresponding author; e-mail: n.torgovkin@yandex.ru*

The results of studies of the ice complex, lacustrine, and lacustrine-alluvial sediments from the Mamontova Gora section performed in 2022–2023 are analyzed. Optically stimulated luminescence dating indicates that the formation of the lacustrine–alluvial sands of the Elga Group ended 250–242 ka ago, at the end of cold MIS 8, while the overlying lacustrine silts accumulated until 138–126 ka ago corresponding to the late cold MIS 6 – early warm MIS 5e. The average isotopic composition of the Yedoma Ice Complex (MIS 3) syngenetic wedge ice is –(31 ± 2)‰ for $\delta^{18}O$, –(239 ± 15)‰ for δD, and (8 ± 2)‰ for $d_{exc}$. For the first time, we quantify the isotopic composition of the Yedoma Ice Complex pore ice with the average values of –(26 ± 2)‰ for $\delta^{18}O$, –(201 ± 17)‰ for δD, and (10 ± 4)‰ for $d_{exc}$. The formation of lacustrine and lacustrine–alluvial sequences during MIS 7 and MIS 5e was fostered by warmer and likely longer thaw periods and associated permafrost thaw. The degree of warming remains to be estimated for this region.

***Keywords:*** *ice complex, lacustrine–alluvial sediments, OSL dating, ground ice, stable oxygen and hydrogen isotopes, paleoclimate, Middle and Late Pleistocene*.

***Recommended citation:*** Torgovkin N.V., Sivtsev D.E., Gavrilova A.A., Platonov I.A., Kizyakov A.I., Schirrmeister L., Opel T., Wetterich S., Breitenbach S.F.M., Meyer H., 2024. New data on the geochronology of Quaternary sediments and stable oxygen and hydrogen isotopes in ground ice of the Mamontova Gora. *Earth's Cryosphere* XXVIII (5), 3–11.

## INTRODUCTION

The Mamontova Gora geological natural monument is a stratotype of the Neogene–Quaternary sediments on the left bank of the Aldan River, 325 km upstream from its junction with the Lena River. The Mamontova Gora section was first described by V.N. Zverev in 1912. In 1915, A.N. Krishtofovich identified American nut fruits in the sediments [*Agadzhanyan et al., 1973*]. From the 1950s, systematic paleobotanic [*Vaskovskiy, Tuchkov, 1953; Baranova et al., 1976*], stratigraphic [*Péwé et al., 1977; Péwé, Journaux, 1983; Alekseev et al., 1990; Kostyukevich, 1993; Minyuk, 2004*], paleontological [*Rusanov, 1968; Vangengeim, 1961, 1977*], sedimentological [*Agadzhanyan et al., 1975; Siegert, 1988*], cryolithological [*Katasonov, Ivanov, 1973*], paleogeographic [*Agadzhanyan et al., 1973; Popp et al., 2006; Vasil'chuk et al., 2019*], and microbiological [*Brouchkov et al., 2017; Cherbunina et al., 2021*] studies of the Mamontova Gora sediments have been conducted. In total, six main geomorphic levels relative to the Aldan River water level have been identified within the geological monument: a high level at 80–90 m above the river level, a 50-m-high terrace, a 30-m-high terrace, a 20-m-high terrace, a 6–9-m-high terrace, and the floodplain [*Agadzhanyan et al., 1973*]. The structure and geochronology of the upper (80–90 m) level and the 50-m-high terrace are shown below (Fig. 1). The genetic types of the sediments are designated by symbols derived from geological maps [*State Geological Map..., 2021*].

Researchers define the geomorphic level of 80–90 m in different ways: as a terrace elevated at 80–100 m above the river [*Vangengeim, 1961; Rusanov, 1968; Péwé, Journaux, 1983*], as a remnant of the watershed surface according to A.A. Svitoch [*Agadzhanyan et al., 1973*], and "as a high (80–90 m) part"

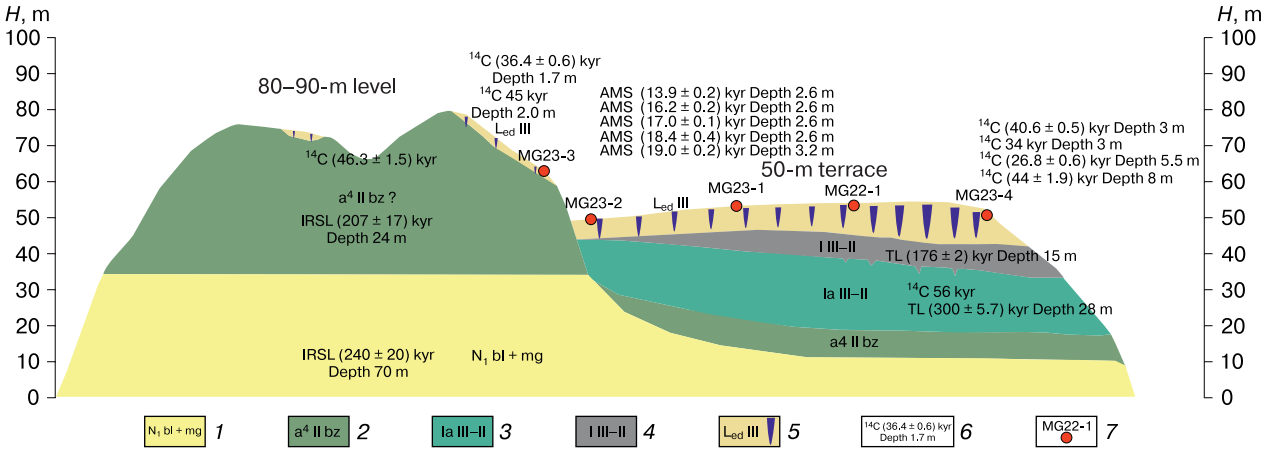


**Fig. 1. Cross-section of the 80–90-m-high level and the 50-m-high terrace of the Mamontova Gora geological natural monument based on maps and sections with dates [*Agadzhanyan et al., 1973; Katasonov, Ivanov, 1973; Kostyukevich, 1993; Vasil'chyuk et al., 2019; Bolshiyanov et al., 2023*].**

*1* – Miocene alluvium, *2* – Bazovskaya formation alluvium; *3* – lacustrine–alluvial sediments; *4* – lacustrine sediments; *5* – ice complex sediments; *6* – dates with sampling depths; *7* – sections studied by the authors.

of Mamontova Gora by M.N. Alekseev [*Alekseev et al., 1990*]. This high level is predominantly composed of variously sized ferruginated cross-bedded sands containing thermophilic Miocene flora: *Juglans cineria* endocarps, *Juglans acuminata* Braun (1845) cones and fruits, *Ulmus* cf. *macrocarpa* Hance (1868) leaves [*Rusanov, 1968; Baranova et al., 1976*]. However, according to the latest data [*Bolshiyanov et al., 2023*], infrared-stimulated luminescence (IRSL) dating of the sands yielded ages of 240 ± 20 kyr at 12 m and 207 ± 17 kyr at 58 m above the Aldan River level. In the upper part of the section, thin (2–3 m) Yedoma Ice Complex (YIC) sediments with ice wedges are fragmentarily exposed in retrogressive thaw slumps [*Voskresensky, 2001*]. Four radiocarbon dates (9–34 ka BP) were obtained from wood in frozen silt at a depth of 1.7–2.0 m during studies conducted by the Geological Institute of the Russian Academy of Sciences, the A.P. Karpinsky All-Russia Geological Research Institute (VSEGEI), and Lomonosov Moscow State University [*Tananaev, 2021*]. The 50-m-high geomorphic level, also called the 50-m terrace (Fig. 1), includes surfaces with relative heights of up to 60–70 m above the river level in elevated areas. It is of particular interest to cryolithologists owing to the prominent exposure of the YIC in these sections. Previous studies have identified a three-layered structure: the lower part (up to 12-m-thick) is attributed to the Zyryansk (Muruktin) Horizon (MIS 4), and the upper part (up to 4-m-thick), is attributed to the Sartan Horizon (MIS 2). A thin (0.5 m) interlayer of peat or peaty loam corresponding to the Kargin Horizon (MIS 3) is sometimes observed between them [*Alekseev et al., 1990; Vasil'chuk et al., 2019; Cherbunina et al., 2021*]. Radiocarbon dates of wood fragments from the YIC sediments are mostly close to the limit of the method [*Tananaev, 2021*]. Accelerator mass spectrometry (AMS) $^{14}C$ dating of organic inclusions in ice wedges (IW) yielded ages of 20–14 kyr BP [*Vasil'chuk et al., 2019*]. The mean values of the isotopic composition of ice wedges are –31 to –28‰ for $\delta^{18}O$ and –237 to –223‰ for $\delta D$ [*Popp et al., 2006; Vasil'chuk et al., 2019*]; the isotopic composition of the pore ice has not been studied yet. A significant amount of the Late Pleistocene fauna remains has been found in the sediments of the 50-m terrace, including *Ursus arctos* (Linnaeus, 1758), *Bison priscus* (Bojanus, 1825), *Alces latifrons* (Johnson, 1874), *Mammuthus primigenius* (Blumenbach, 1799), *Rangifer tarandus* (Linnaeus, 1758), *Coelodonta antiquitatis* (Blumenbach, 1799), *Equus caballus* (Linnaeus, 1758) and *Panthera spelaea* (Goldfuss, 1810) [*Rusanov, 1968*]. The genesis of the YIC remains a subject of debate. Different hypotheses have been proposed: cryogenic aeolian [*Rusanov, 1968; Péwé, Journaux, 1983*]; alluvial–permafrost [*Agadzhanyan et al., 1975*]; polygenetic [*Siegert, 1988; Schirrmeister et al., 2013*]. On the current 1:1,000,000-scale Map of Quaternary Deposits, these formations are marked as cryogenic–aeolian formations – loessoids [*State Geological Map..., 2021*]. The YIC is imbedded into lacustrine and alluvial–lacustrine loamy sands with the thermoluminescence (TL) age of 176 ± 2 kyr [*Katasonov, Ivanov, 1973*]. Cones of *Larix dahurica* Turcz. and *Picea obovata* Ldb. were found in these sediments. An approximately equal proportion of pollen from the tree and shrub species *Betula* sect. *Nanae, B.* sect. *Fruticosae, Alnaster*; less *Pinus, Alnus, Betula* sect. *Albae*; herbs Caryophyllaceae and others; and spores of *Bryales, Sphagnum,* Polypodiaceae, and *Se-*

*laginella* has been established [*Alekseev et al., 1990*]. These sediments are underlain by lacustrine–alluvial sands of the Elginskaya formation with the TL age of 300 ± 5.7 kyr [*Katasonov, Ivanov, 1973; Kostyukevich, 1993*]. The palynocomplex of the Elginskaya formation is represented by trees and shrubs (*Pinus, Picea, Betula* sect. *Albae, B.* sect. *Nanae, B.* sect. *Fruticosae, Alnus, Alnaster*), spores (Polypodiaceae, *Sphagnum, Bryales),* and herbs (Polygonaceae, *Artemisia*) [*Alekseev et al., 1990*]. At the base, there is a layer of alluvial basal gravels of the Bazovskaya formation containing pollen of trees (*Pinus, Picea, Larix, Betula, Alnus*), shrubs (*Alnaster* and Ericales), and herbs (*Artemisia,* Gramineae, Polygonaceae) and spores (*Bryales,* Polypodiaceae, *Sphagnum, Lycopodium*) and ferruginated alluvial Miocene sands [*Alekseev et al., 1990*]. Despite decades of research on the sections of Mamontova Gora, the following questions remain unresolved: (a) exact time of formation of Quaternary lacustrine and lacustrine–alluvial sediments and (b) paleoclimatic conditions of the YIC formation.

## Field and laboratory research methods

Field and laboratory methods were selected based on the features of the studied object and the established scientific goals.

*Cryolithological description.* During the 2022 and 2023 field seasons, some fragments of the sections of the 50-m terrace and the 80–90-m level were studied. In the upper part of the 50-m terrace, sections were described and sampled, including samples of the YIC in the walls of small thaw slumps (thermocirques) (Fig. 2; points MG22-1, MG23-1, MG23-2). A thermocirque with an YIC exposure was found and studied on a lowered remnant of the 80–90-m level (Fig. 2, point MS23-3). The studied sections were described in terms of their lithological and cryogenic structure [*Zhestkova et al., 1980*] and samples were taken from: (a) ice wedges and pore ice for determining the isotopic composition; (b) sediments of the YIC, slope cover, lacustrine, and lacustrine–alluvial horizons. In the middle part of the 50-m terrace, a series of excavations of lacustrine and lacustrine–alluvial sediments was performed to describe their morphology and determine their age (Fig. 2, point MG23-4).

*Optically stimulated luminescence (OSL) dating* is based on the release of the luminescence signal from grains of quartz and/or feldspar in the sand and coarse silt fractions. Dating of Quaternary deposits was completed by the only OSL laboratory in Russia – at the Karpinsky All-Russia Geological Research Institute in St. Petersburg.

*Determination of stable isotopes* $\delta^{18}O$, $\delta D$ *and of* $d_{exc}$ *in ground ice.* Ice wedges are studied as archives of the climatic conditions of the Pleistocene and Holocene on the Arctic coast of Russia, northeastern Siberia, Alaska, and Canada. In turn, studies of pore ice

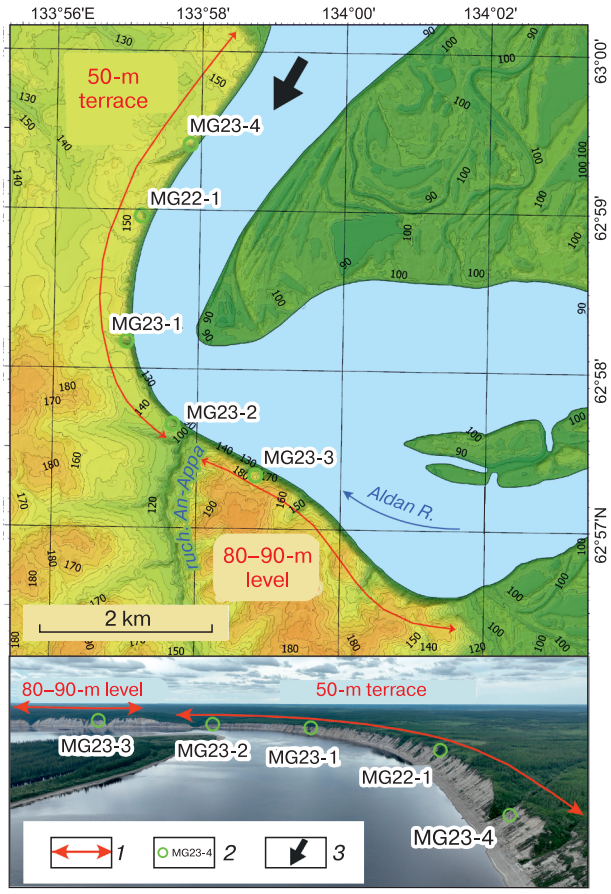


**Fig. 2. Location of the sampled sections on the terrace scarps of the Mamontova Gora geological natural monument.**

*1* – length of the 50-m terrace and the 80–90-m level along the Aldan River, *2* – sampled sections, *3* – geoposition and direction of aerial perspective photography.

in syngenetic deposits allows us to characterize the conditions of freezing in the active layer [*Meyer et al., 2002; Derevyagin et al., 2013; Porter, Opel, 2020*]. To identify moisture conditions, deuterium excess ($d_{exc}$) is used, which is calculated as $d_{exc} = \delta D - 8 \cdot \delta^{18}O$. If it is equal to 8, the conditions are considered meteoric; if lower, evaporation prevails; if higher, then we assume additional water condensation [*Dansgaard, 1964*]. Ice wedge samples were taken along a horizontal profile, and pore ice samples were taken along a vertical profile using a cordless drill with a cylindrical attachment. The sampling locations were cleaned beforehand to avoid contaminating the sample with melt water. The ice samples were collected and thawed in zip bags at ambient temperature of around 25°C. After complete thawing, the samples were poured into polyethylene 15-mL test tubes for transport to the laboratory. Laboratory isotope analysis of the ground ice samples was completed on a Picarro

L-2140i high-precision isotopic analyzer in the joint Russian–German (MPI-AWI Potsdam) isotope laboratory at the Melnikov Permafrost Institute, Siberian Branch of the Russian Academy of Sciences, Yakutsk.

## RESULTS

### Geological description of the sections of Quaternary sediments underlying the Yedoma Ice Complex

At section **MG23-4** (62°59′24.1″ N, 133°57′50.5″ E), a series of outcrops exposed Quaternary and Miocene sediments underlying the YIC in the middle part of the 50-m terrace with a total exposure height of 55 m at the wall of a V-shaped gully (Fig. 3). The genetic types of sediments are designated by symbols in accordance with the state geological map legend [*State Geological Map..., 2021*].

From bottom to top, the following layers are exposed in the section: *Miocene alluvium – Belogorsk layers – Mamontova Gora formation* ($N_1$ bl-mg), ferruginated white and gray sands with diagonal bedding; their thickness reaches 15–16 m.

*Alluvium of the fourth fluvial terrace – Bazovskaya formation* ($a^4$II bz) lies unconformably on the Miocene sands. It consists of ferruginated gravels with sandy and silty fill; approximately 10 m in thickness.

*Lacustrine–alluvial sediments of the Elginskaya formation* (la II–III el) conformably overlie gravels of the Bazovskaya formation. In the interval of 26–32 m above the river level, the section consists of medium- to coarse-grained gray sand of the channel facies with horizontal bedding and cross-bedding (30°–45°). At the heights of 33, 36, and 38 m, brown-gray silt layers of up to 0.5 m in thickness were described. At the height of 39 m, this layer is overlain by the layer of medium and coarse-grained white-gray sands with ferruginated gravel lenses. At a height of 38–39 m, a pseudomorph was found, representing the tail of a melted ice wedge. The pseudomorph is composed of lacustrine silts lying above and strongly ferruginated sands. At a height of 38.5 m, the OSL age of the sands is 250 ± 36 kyr; and at a height of 37 m, it is 242 ± 34 kyr.

The formation of the lacustrine–alluvial deposits of the Elginskaya formation, which is the stratigraphic counterpart of the Mavrinskaya formation in the middle reaches of the Lena River, corresponds to the end of the MIS 8 glacial–the beginning of the MIS 7 interglacial, which took place 243–191 kyr BP. This period saw permafrost degradation across southern Siberia, evidenced by speleothem growth in Botovskaya Cave [*Vaks et al., 2013, 2020*].

*Lacustrine sediments* (l II–III) lie on lacustrine–alluvial sands of the Elginskaya formation (39–49 m) and are represented by gray dense silts with traces of gleying in the form of irregularly shaped bluish mottles and evenly distributed multidirectional lenticular ocherous iron-rich mottles. The sediments contain rare charcoal inclusions and have a reticulate cryogenic structure. The OSL age of the silts is 138 ± 15 kyr at a height of 47 m and 126 ± 11 kyr at a height of 46.5 m.

These lacustrine sediments were likely deposited 130–115 kyr ago at the end of MIS 6 glacial–beginning of MIS 5e interglacial. This interval was marked by extensive permafrost thaw, speleothem formation in Botovskaya Cave [*Vaks et al., 2013, 2020*] and the formation of a woody horizon at the Batagay megaslump [*Murton et al., 2023*].

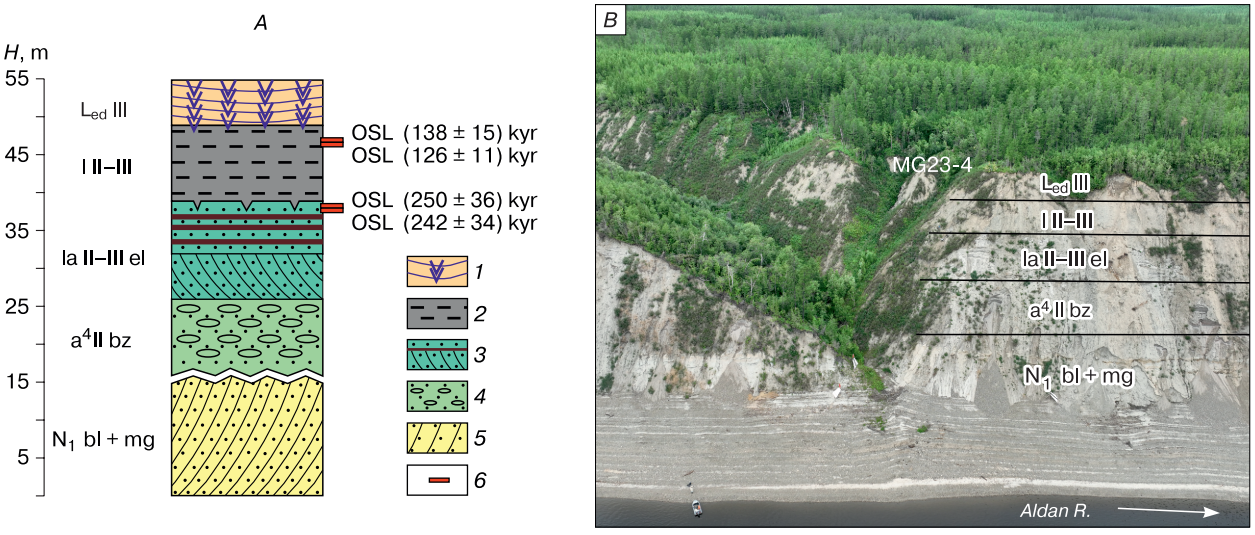


**Fig. 3. Sediments composing 50-m-high terrace of Mamontova Gora at section MG23-4.**

*A* – structure of section MG23-4 with OSL dates; *B* – overall view of of the exposure. *1* – ice complex, *2* – lacustrine sediments, *3* – lacustrine–alluvial sediments, *4* – alluvial sediments of Bazovskaya formation, *5* – Miocene alluvium, *6* – points of sampling for OSL dating.

*Yedoma Ice Complex* ($L_{ed}$ III) in this section consists of thawed and slumped gray-brown silts with patches of iron concentrations, fragments of tree rootlets and twigs, thread-like rootlets of grasses, and charcoals. The visible thickness is 6 m (at a height of 49–55 m). A more detailed description of the YIC is provided below.

### Structure of Yedoma Ice Complex sections

Section **MG22-1** (62°58′57.7″ N, 133°57′09.8″ E; 58 m above the river level; wall of the north-north-eastern aspect) is located on the 50-m terrace (Figs. 4*A*–4*C*). The YIC sediments are exposed on the side of a short gully cutting the bottom of a large

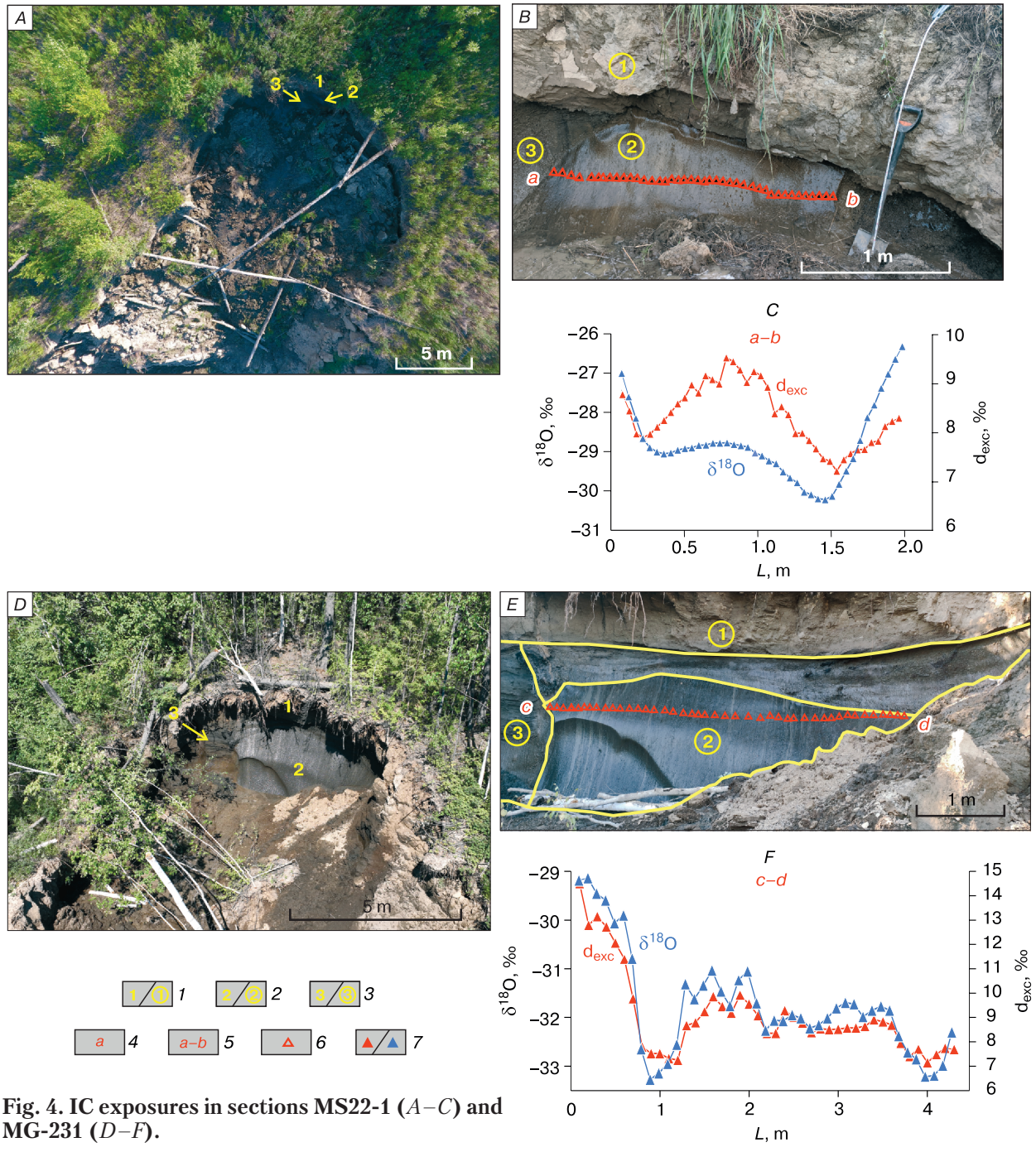


**Fig. 4. IC exposures in sections MS22-1 (*A*–*C*) and MG-231 (*D*–*F*).**

*A*, *D* – types of thermocirques at the top; *B*, *E* – exposed ice wedge fragments with sampling profiles *a*–*b* and *c*–*d*; *C*, *F* – isotopic composition ($\delta^{18}O$) and deuterium excess ($d_{exc}$) of ice wedge samples from profile *a*–*b* and *c*–*d*. *1* – brown-gray silty layer overlaying the YIC, *2* – ice wedge, 3 – ground column of the YIC, *4* – beginning of the profile, *5* – profiles, *6* – sampling points of syngenetic ice wedges, *7* – isotopic composition ($\delta^{18}O$) and deuterium excess ($d_{exc}$) of ice wedge samples.

thaw slump around 300 m in diameter. The height difference from the edge of the thaw slump to the sampling point MG22-1 is 10–12 m, and consequently, approximately this thickness of the upper part of the YIC was previously removed by thermal denudation. In the studied outcrop, in the rear wall of a small thaw slump of about 10 m in diameter, a fragment of the YIC sediments is exposed, covered by a two-meter layer of slope material that was displaced to the bottom of the thaw slump during the period of its active growth. The YIC exposure of about 1 m in height and 15 m in width includes fragments of a syngenetic ice wedge and a sediment column. The sediment column is composed of frozen gray brown silt with layered cryogenic structure and inclusions of thread-like rootlets and wood fragments. The ice wedge has vertical striation, the width of the elementary veins is 2–4 mm. The isotopic composition of the ice wedge is shown in Fig. 4*C*.

Section **MG23-1** (62°58′10.4″ N, 133°56′57.6″ E, 54–58 m above the river level; wall of the southern aspect). A small thermocirque is located at the edge of the left wall of the gully flowing into the Aldan River (Figs. 4*D*–4*F*). The YIC sediments with a fragment of a syngenetic ice wedge exposed at an angle to its axis are seen on an 8-m-wide exposure. The right contact of the ice wedge with host sediments is covered by slumped material. The width of the ice wedge in the exposure wall is 4 m, the height is 2 m. The YIC sediments are covered by slope deposits – a 1.5-m-thick layer of brown-gray silt. The YIC sediments composing the sediment column between the ice wedges are represented by gray and brownish gray silt with a thin-layered cryostructure with subhorizontal ice lenses of 0.1 mm in thickness and vertical distances between them of 0.2–3.0 mm. The YIC sediments contain abundant thread-like rootlets. The isotopic composition of the ice wedges sampled along the horizontal profile is shown in Fig. 4*F*.

Section **MG23-2** (62°57′37.7″ N, 133°57′42.7″ E; 34 m above the river level; wall of the north-northeastern aspect). A small thaw slump (thermocirque) at the edge of the terrace on the left high bank of the Aldan River is located 120 m downstream from the mouth of the An-Appa River (Fig. 2; Figs. 5*A*–5*C*). The low (1–2 m) rear wall of the thermocirque gradually passes into the inclined bottom dissected by erosional cuts near the edge of the terrace. In the rear wall of the thermocirque, a layer of the YIC with a visible thickness of 4–5 m is fragmentarily exposed, and the lower part of the syngenetic ice wedges is exposed in the sloping bottom of the thermocirque.

The top surface of the syngenetic ice wedge in the YIC is located at a depth of 1.9 m. The width of the wedge is 3 m, and its height is about 5 m. From the edge of the exposure to a depth of 0.95 m, there is a layer of highly plastic loam with inclined layered and wavy cryostructure repeating the slope of the bottom, with ice lenses (1–7 mm) spaced apart at 4–8 mm in the vertical section. Below 0.95 m, there is loam with a reticulate cryostructure with mineral blocks of up to 4–14 mm surrounded by 3–4-mm-thick ice lenses and a single 30-mm-thick ice band. This loam is underlain by the loam with reticulate cryostructure and ice lenses of 2–5 mm in thickness; it lies atop the upper surface of the ice wedge. At a depth of about 1 m, directly under the ice band, a 0.4-m-wide head of a narrower and younger ice wedge (presumably, epigenetic) is seen. Its tail penetrates the head of the wide syngenetic ice wedge of the YIC. The isotopic composition of the syngenetic ice wedge is shown in Fig. 5*C*.

Section **MG23-3** (62°57′21.1″ N, 133°58′50.1″ E; 64–66 m above the river level; wall of the north-northwestern aspect). Within the area of the 80–90-m level along the Aldan River (Fig. 2), there is a lowered fragment with the height of 64–68 m above the river level. A thermocirque of about 15 m in diameter with exposed YIC sediments (Figs. 5*D*–5*F*) is cut into the edge of this section. In the walls of the thermocirque with a height of 2.1 to 4 m in an inclined section, two YIC ice wedges of up to 3.8 m in width and a soil column separating them are exposed. Samples were taken from the ice wedge; we also sampled pore ice from the host sediments (Figs. 5*E*, 5*F*). Wedge ice is dissected by an inclined 8-cm-thick interlayer of loesslike loam with a massive cryostructure in the upper part of layered cryostructure in the lower part (ice lenses of 2–4 mm separated by mineral interlayers of 4–8 mm (Fig. 5*F*). The orientation of ice veins in the ice wedge is similar below and above the interlayer of the loesslike loam. Two sampling profiles across the ice wedge were completed (Fig. 5*F*).

The YIC formed in several stages during MIS 4–2, which is confirmed by numerous radiocarbon dates ranging from 56 to 14 kyr BP [*Péwé et al., 1977; Péwé, Journaux, 1983; Popp et al., 2006; Vasil'chuk et al., 2019; Tananaev, 2021*]. The YIC was formed in cold and arid climatic conditions of the Late Pleistocene, which is confirmed by the light isotopic composition of the wedge ice and pore ice (Fig. 6).

The average isotopic composition of the syngenetic ice wedges (−31 ± 2‰ for $\delta^{18}O$ and −239 ± 15‰ for δD) is generally similar to previously published data on the Late Pleistocene ice wedges from Mamontova Gora [*Popp et al., 2006; Vasil'chuk et al., 2019*]. The isotopic composition of pore ice varies widely: −31.7 to −21.9‰ for $\delta^{18}O$; −247.5 to −162.6‰ for δD; and 3 to 18‰ for $d_{exc}$.

The most complete profile of pore ice was sampled at point MG23-3 (Fig. 5*E*), where a gradual decrease of the isotopic composition and increase in $d_{exc}$ can be traced upward the section. The same trend is seen in the isotopic composition of the layered cryostructure at point MG22-1. The opposite trend, with the isotopic composition becoming heavier upward

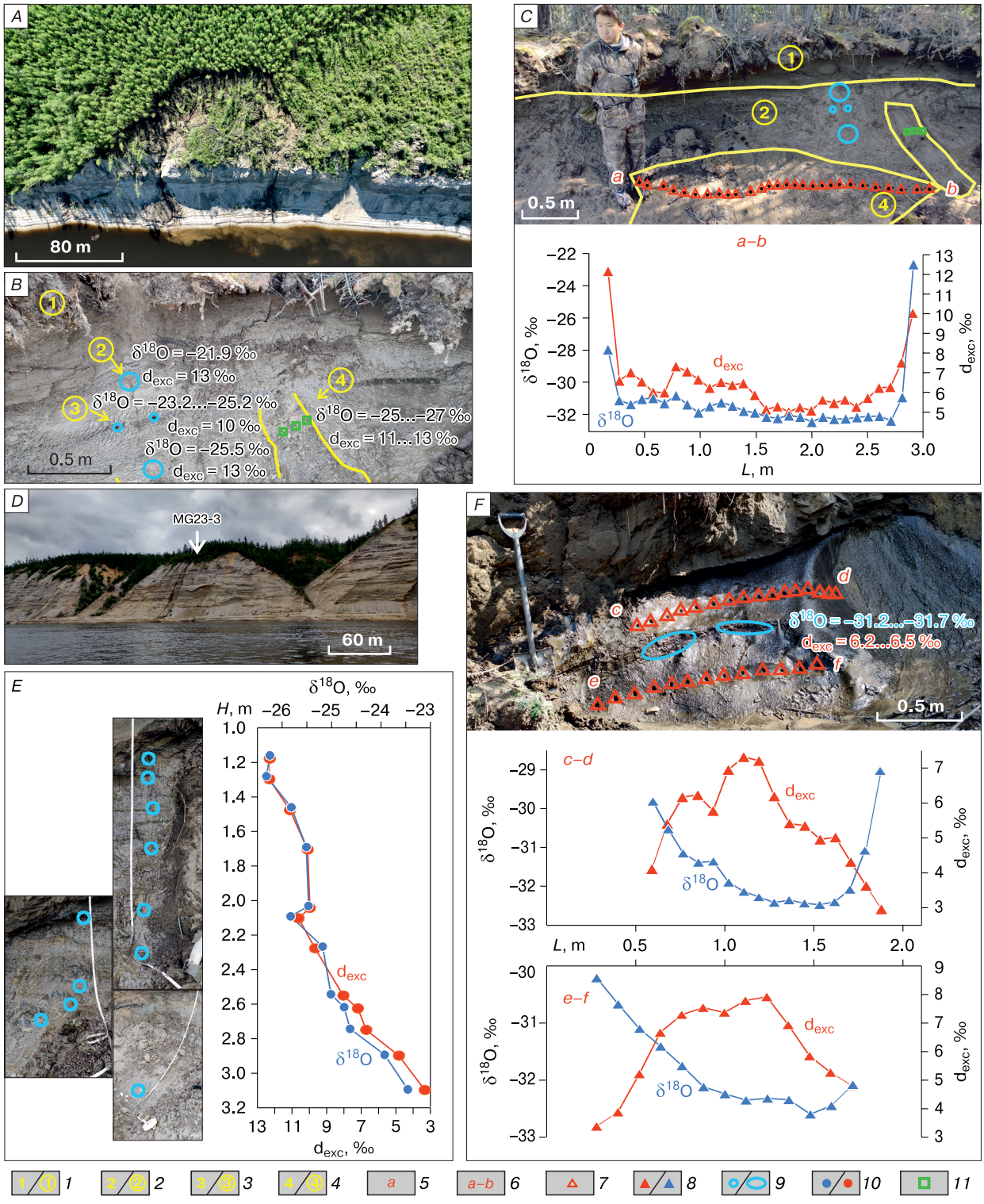


**Fig. 5. Outcrops of the YIC in sections MG23-2 (*A*–*C*) and MG23-3 (*D*–*F*).**

*A* – view of thermocirque from the top; *B*, *C*, *F* – exposed segments of ice wedges with sampling profiles *a*–*b*, *c*–*d*, and *e*–*f* and isotopic composition ($\delta^{18}O$) and deuterium excess ($d_{exc}$) data on ice wedge samples along the profiles; *D* – view of the thermocirque from the river; *E*, *F* – schemes of ice sampling and isotopic composition ($\delta^{18}O$) and deuterium excess ($d_{exc}$) data for (*E*) pore ice and wedge ice (*F*). *1* – layer of brown-gray silt overlaying the YIC sediments; *2* – sediments atop the ice wedge; *3* – large ice lens in the frozen ground column; *4* – ice wedge; *5* – beginning of the profile; *6* – sampling profiles; *7* – sampling points of syngenetic ice wedges, *8* – isotopic composition ($\delta^{18}O$) and deuterium excess ($d_{exc}$) of ice wedge samples, *9* – points of pore ice sampling; *10* – isotopic composition ($\delta^{18}O$) and deuterium excess ($d_{exc}$) of pore ice; *11* – sampling points from a narrow and younger, supposedly, epigenetic ice vein.

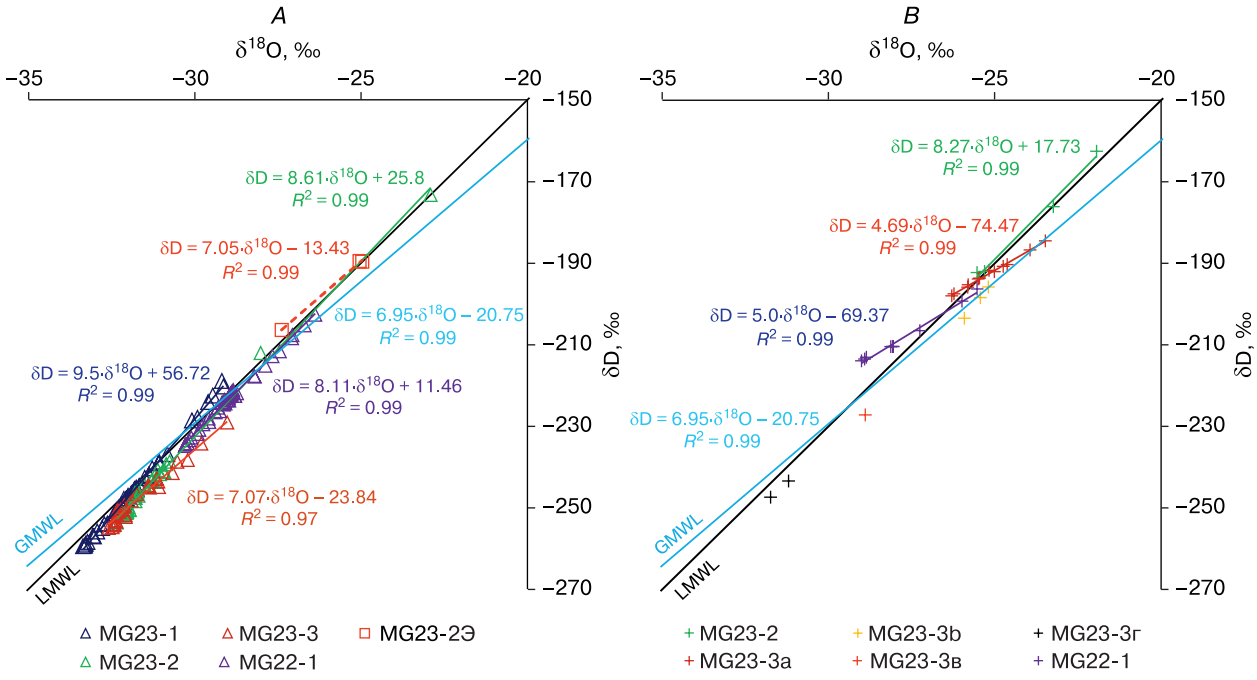


**Fig. 6. Isotopic composition ($\delta^{18}O$ and $\delta D$) of ground ice with linear regression equations relative to the Global Meteoric Water Line (GMWL) and the Local Meteoric Water Line (LMWL) [*Papina et al., 2017*].**

*A* – ice wedges; *B* – pore ice.

through the section, is observed in the pore ice of MG23-2 (Fig. 5*B*), which is located closer to the surface than the others.

Pore ice is formed by water from the lower part of the active layer, which passes into the permanently frozen state in the course of the accumulation of sediments and syngenetic freezing. Presumably, isotopic fractionation associated with periodic thawing and freezing of the transient layer has a certain influence. Pore ice in section MG23-3 lying closer to the surface has the lightest isotopic composition and high $d_{exc}$; conversely, pore ice lying deeper has a heavier isotopic composition and low $d_{exc}$ (Fig. 5*F*). Low slopes in linear regression equations equal to 4.7 (MG23-3) and 5 (MG22-1) for pore ice (Fig. 6*B*) indicate changes in the isotopic composition of the original atmospheric water due to fractionation during freezing, thawing, and frost desiccation of the YIC soil column. The trend towards lighter isotopic composition upward in the section may be associated with changes in surface paleoecological and climatic conditions during the transition from a warmer MIS 3 to a colder MIS 2. In the absence of dating of the studied sediments, it is impossible to confirm this hypothesis. A similar tendency towards lighter isotopic composition of pore ice and wedge ice during the transition from MIS 3 to MIS 2 was recorded in the YIC of the Laptev Sea coast at the Mamontov Klyk and Oyogoss Yar exposures and on Bolshoy Lyakhovsky Island [*Derevyagin et al., 2013, 2016*].

## CONCLUSIONS

It has been found that the formation of lacustrine–alluvial sediments of the Elginskaya formation and the overlying lacustrine sediments occurred during the transitions from glacial to interglacial periods MIS 8–MIS 7 and MIS 6–MIS 5e, respectively, under conditions of the long-term thawing from the surface.

Preliminary data on the isotopic composition of pore ice of the YIC from the 50-m terrace and the 80–90-m level showed a significant influence of cryogenic fractionation of the original atmospheric water during the freeze–thaw processes. The linear trend of changes in the isotopic composition of pore ice with depth in the YIC section may be a marker of directional changes in the paleoclimatic conditions of sediment accumulation, characteristic of the transition from the warm and humid climate of MIS 3 to the cold and arid climate of MIS 2.

For the first time, OSL dating has been performed for lacustrine (138–126 kyr) and lacustrine–alluvial (250–242 kyr) sediments of the Elginskaya formation exposed in the 50-m terrace of Mamontova Gora. These results provide absolute age constraints and offer new insights into the Quaternary depositional history of the eastern part of Central Yakutia.

***Acknowledgements.*** *This work was funded by the Head of the Sakha Republic's Grant for Young Scientists, Specialists and Students no. 122012800064-9*

*"The Construction and Key Stages of the Evolution of the Continental Cryolithozone in the Late Pleistocene and Holocene". A.I. Kizyakov participated in these works within the framework of state assignment "The Evolution of the Cryosphere under Climate Change and Anthropogenic Impact" (no. 121051100164-0).*

## References

Agadzhanyan A.K., Boyarskaya T.D., Glushankova N.I., Shlyukov A.I., 1973. *Section of the Latest Sediments of Mamontova Gora*. Moscow, Izd. Mosk. Gos. Univ., 173 p. (in Russian)

Agadzhanyan A.K., Boyarskaya T.D., Glushankova N.I. et al., 1975. Section of the latest sediments of Mamontova Gora. In: *Paleogeography and Periglacial Phenomena of the Pleistocene*. Moscow, Izd. Mosk. Gos. Univ., p. 40–49. (in Russian)

Alekseev M.N., Grinenko O.V., Kamaletdinov V.A., Mochanov Y.A., 1990. *Neogene and Quaternary Sediments of the Lower Aldan Depression and the Middle Lena (Central Yakutia). Guidebook of Geologic Excursions (Yakutsk, July 12–21, 1990)*. Yakutsk, Yakutsk Sci. Center Publ., 42 p. (in Russian)

Baranova Yu.P., Ilyinskaya I.A., Nikitin V.P. et al., 1976. *Miocene of the Mamontova Gora Outcrop (Stratigraphy and Fossil Flora)*. Moscow, Nauka, 284 p. (in Russian)

Bolshiyanov D.Yu., Pravkin S.A., Fomenko A.P. et al., 2023. Study of the section of Quaternary sediments of Mamontova Gora on the Aldan River. In: *Relief and Quaternary Deposits of the Arctic, Subarctic, and North-West Russia* (Conf. Proc.), Iss. 10, p. 30–35. (in Russian)

Brouchkov A., Kabilov M., Filippova S., Baturina O., Rogov V., Galchenko V., Mulyukin A., Fursova O., Pogorelko G., 2017. Bacterial community in ancient permafrost alluvium at the Mammoth Mountain (Eastern Siberia). *Gene* **636**, 48–53.

Cherbunina M.Y., Karaevskaya E.S., Vasil'chuk Y.K. et al., 2021. Microbial and geochemical evidence of permafrost formation at Mamontova Gora and Syrdakh, Central Yakutia. *Frontiers Earth Sci.* **9**, 739365.

Dansgaard W., 1964. Stable isotope in precipitation. *Tellus* **XVI** (4), 436–468.

Derevyagin A.Yu., Chizhov A.B., Meyer H. et al., 2013. Isotopic composition of texture ice of the Laptev Sea coast. *Kriosfera Zemli* XVII (3), 27–34. (in Russian)

Derevyagin A.Yu., Chizhov A.B., Meyer H., Opel T., 2016. Comparative analysis of the isotopic composition of ice wedges and texture ices at the Laptev Sea coast. *Earth's Cryosphere* XX (2), 14–22.

Katasonov E.M., Ivanov M.S., 1973. *Cryolithology of Central Yakutia. Guide to the Excursion Along the Lena and Aldan* (II Int. Conf. on Permafrost): Proc., Yakutsk, Izd. OUPES SO AN SSSR, 37 p. (in Russian)

Kostyukevich V.V., 1993. A regional geochronological study of Late Pleistocene permafrost. *Radiocarbon* **35** (3), 477–486.

Meyer H., Siegert C., Derevyagin A. et al., 2002. Paleoclimate reconstruction on Big Lyakhovsky Island, North Siberia – hydrogen and oxygen isotopes in ice wedges. *Permafr. Periglac. Process.* **13**, 91–103.

Minyuk P.S., 2004. *Magnetostratigraphy of the Cenozoic of the Northeast of Russia*. Magadan, SVKNII FEB RAS, p. 198. (in Russian)

Murton J., Opel T., Wetterich S., Ashastina K., Savvinov G., Danilov P., Boeskorov V., 2023. Batagay Megaslump: a review of the permafrost deposits, quaternary environmental history, and recent development. *Permafr. Periglac. Process.* **34** (3), 399–416.

Papina T.S., Malygina N.S., Eirikh A.N. et al., 2017. Isotopic composition and sources of atmospheric precipitation in Central Yakutia. *Earth's Cryosphere* XXI (2), 52–61. (in Russian)

Péwé T., Journaux A., 1983. Origin and character of loesslike silt in unglaciated Southern and Central Yakutia, Siberia, U.S.S.R. *Geol. Survey Profess. Paper* **1262**, 1–45.

Péwé T., Journaux A., Stuckenrath R., 1977. Radiocarbon dates and Late Quaternary stratigraphy from Mamontova Gora, unglaciated Central Yakutia, Siberia, U.S.S.R. *Quat. Res.* **8** (1), 51–63.

Popp S., Diekmann B., Meyer H. et al., 2006. Palaeoclimate signals as inferred from stable-isotope composition of ground ice in the Verkhoyansk Foreland, Central Yakutia. *Permafr. Periglac. Process.* **17** (2), 119–132.

Porter T.J., Opel T., 2020. Recent advances in paleoclimatological studies of arctic wedge- and pore-ice stable-water isotope records. *Permafr. Periglac. Process.* **31** (3), 429–441.

Rusanov B.S., 1968. *Biostratigraphy of Cenozoic sediments of Southern Yakutia*. Moscow, Nauka, 459 p. (in Russian)

Schirrmeister L., Froese D., Tumskoy V. et al., 2013. Yedoma: Late Pleistocene Ice-Rich Syngenetic Permafrost of Beringia. In: *The Encyclopedia of Quaternary Science*, vol. **3**, 542–552.

Siegert C.G., 1988. Mineralogical and petrographic characterization of sediments of ice complexes of Central Yakutia. In: *Problems of Geocryology*. Moscow, Nauka, p. 101–107. (in Russian)

State Geologic Map of the Russian Federation on a Scale of 1:1 000 000. Third Generation, 2021. Verkhoyan–Kolyma series. Sheet P-53 Khandyga. Explanatory note (Kazakova G.G., Tutasova E.N., Khudoley A.K. et al.). St. Petersburg, VSEGEI Publ., 431 p. + 8 Suppl. (in Russian).

Tananaev N., 2021. *Radiocarbon Dates from Central Yakutia*. Dataset, vol. 31. – https://doi.org/10.6084/m9.figshare.14261372.v2

Vaks A., Gutareva O.S., Breitenbach S.F.M., Avirmed E., Mason A.J., Thomas A.L., Osinzev A.V., Kononov A.M., Henderson G.M., 2013. Speleothemes reveal 500 000-year history of Siberian permafrost. *Science* **340**, 183–186.

Vaks A., Mason A.J., Breitenbach S.F.M., Kononov A.M., Osinzev A.V., Rosensaft M., Borshevsky A., Gutareva O.S., Henderson G.M., 2020. Paleoclimate evidence of vulnerable permafrost during times of low sea ice. *Nature* **577**, 221–225.

Vangengeim E.A., 1961. Paleontological Substantiation of the Stratigraphy of Anthropogene Deposits in the North of Eastern Siberia (on Mammals). In: *Tr. Geol Inst. Akad Nauk SSSR*, Iss. 48. Moscow, Izd. Akad. Nauk SSSR, 189 p. (in Russian)

Vangengeim E.A., 1977. *Paleontological Substantiation of the Stratigraphy of the Anthropogene of Northern Asia (On Mammals)*. Moscow, Nauka, 172 p. (in Russian)

Vasil'chuk Y.K., Shmelev D.G., Cherbunina M.Y. et al., 2019. New isotope-oxygen diagrams of Late Pleistocene and Holocene ice wedges in Mamontova Gora and Syrdakh Lake, Central Yakutia. *Dokl. Earth Sci.* **486**, 580–584.

Vaskovskiy A.P., Tuchkov I.I., 1953. Solution of the most important paleoenvironment problem of Mamontova Gora, Aldan River. *Kolyma* 9, 42–44. (in Russian)

Voskresensky K.S., 2001. *Modern Relief-Forming Processes on the Plains of Northern Russia*. Moscow, Geogr. Faculty, Moscow State Univ., 262 p. (in Russian)

Zhestkova T.N., Zabolotskaya M.I., Rogov V.V., 1980. *Cryogenic Structure of Frozen Rocks*. Moscow, Izd. Mosk. Gos. Univ., 137 p. (in Russian)

*Received May 6, 2024*
*Revised July 4, 2024*
*Accepted August 25, 2024*
*Translated by M.A. Korkka*